45TH TURBOMACHINERY & 32ND PUMP SYMPOSIA
HOUSTON, TEXAS | SEPTEMBER 12 – 15, 2016
GEORGE R. BROWN CONVENTION CENTER

EFFECT OF RELATIVE JOURNAL BEARING AND HONEYCOMB SEAL DIRECT STIFFNESS ON RADIAL SYNCHRONOUS VIBRATIONS OF HIGH-PRESSURE CENTRIFUGAL COMPRESSORS

Leonardo Baldassarre
Engineering Executive for Compressors and Auxiliary Systems
GE Oil & Gas
Florence, Italy

Michele Fontana
Engineering Manager for Centrifugal Compressors
GE Oil & Gas
Florence, Italy

Andrea Bernocchi
Senior Engineering Manager for Centrifugal Compressors
GE Oil & Gas
Florence, Italy

Michele Moretti
Centrifugal Compressor Design Engineer
GE Oil & Gas
Florence, Italy

Leonardo Baldassarre is currently Engineering Executive Manager for Compressors and Auxiliary Systems with GE Oil & Gas, in Florence, Italy. He is responsible for requisition and standardization activities and for the design of new products for compressors, turboexpanders and auxiliary systems.
Dr. Baldassarre began his career with GE in 1997. He worked as Design Engineer, R&D Team Leader, Product Leader for centrifugal and axial compressors and Requisition Manager for centrifugal compressors.
Dr. Baldassarre received a B.S. degree (Mechanical Engineering, 1993) and Ph.D. degree (Mechanical Engineering / Turbomachinery Fluid Dynamics, 1998) from the University of Florence. He authored or coauthored 20+ technical papers, mostly in the area of fluid dynamic design, rotating stall and rotordynamics. He presently holds five patents.

Andrea Bernocchi is an engineering manager at GE Oil & Gas. He joined GE in 1996 as Centrifugal Compressor Design Engineer after an experience in plastic machinery industry. He has 18 years of experience in design development, production and operation of centrifugal compressor. He covered the role of LNG compressor design manager for 6 years with responsibility in design of LNG compressors, testing and supporting plant startup. He's currently leading the requisition team for centrifugal and axial compressor design.
Mr. Bernocchi received a B.S. degree in Mechanical Engineering from University of Florence in 1994. He holds 4 patents in compressor field.

Michele Fontana is currently Engineering Manager for Centrifugal Compressor Upstream, Pipeline and Integrally Geared Applications at GE Oil & Gas, in Florence, Italy. He supervises the calculation activities related to centrifugal compressor design and testing, and has specialized in the areas of rotordynamic design and vibration data analysis.
Mr. Fontana graduated in Mechanical Engineering at University of Genova in 2001. He joined GE in 2004 as Centrifugal Compressor Design Engineer, after an experience as Noise and Vibration Specialist in the automotive sector.
He has co-authored nine technical papers about rotordynamic analysis and vibration monitoring, and holds two patents in this same field.

Michele Moretti is currently Centrifugal Compressor Design Engineer at GE Oil & Gas, in Florence, Italy. His current duties are mainly focused on rotordynamic and thermodynamic design and testing of Centrifugal Compressors for High Pressure Upstream and Pipeline Applications.
He joined GE in 2014 as Centrifugal Compressor Design Engineer, after an experience as dynamic specialist in the helicopter industry.
Mr. Moretti received a Master degree in Aerospace Engineering from University of Pisa in 2009.

ABSTRACT

High pressure compressors are commonly equipped with honeycomb seal on the balance piston, as an effective mean to improve the rotordynamic stability of the system. The gas leakage flow across the honeycomb seal clearance develops significant stiffness and damping effects, that have been extensively studied and experimentally measured in the past.

When the differential pressure across the honeycomb seal is very high, the magnitude of the stiffness and damping synchronous coefficients associated to the seal may become comparable to those of the journal bearings. These additional coefficients cause significant variations of the rotordynamic behavior of the compressor with respect to the no-load case, altering the frequency, amplification factor and mode shape of the natural modes of the system. This has a direct impact on the radial vibrations of the rotor that needs to be evaluated during the design phase of the machine.

The present study describes the above mentioned aerodynamic effects, analyzing their impact on compressor rotordynamics as well as their dependence on influencing parameters such as the stiffness ratio between honeycomb seal and journal bearings. The analysis is supported by experimental data measured on two high pressure compressors (550 bar final discharge) with similar geometry and operating conditions but different journal bearing configuration. Conclusions include some recommendations about the design of the honeycomb seal and of the journal bearings, based on the outcome of the analysis and on the presented experimental results.

INTRODUCTION

Rotor-stator seals and rotordynamic stability

The flowpath portion of a centrifugal compressor is equipped with a set of gas annular seals to minimize the flow recirculation between compression stages, which has a significant impact on the overall efficiency of the compressor. Labyrinth seals are most commonly applied on impellers, spacers and balance drums. Starting from several decades ago (Wachel, 1975), studies showed that the aerodynamic effects associated to these seals may generate destabilizing effects on the rotor, basically due to the rotation of the annular gas volume enclosed between the seal and rotor surfaces.

A radial displacement ***r*** of the rotor from the seal axis is associated to a reaction force ***F*** due to the interaction with the gas volume; this behavior is modeled in Equation (1), with the aid of a stiffness matrix *[K]* and a damping matrix *[C]* assumed to be skew-symmetric (for a detailed presentation of such a model see for example Muszynska, 2005, p.232). *x* and *y* are the horizontal and vertical components of the rotor radial displacement ***r***.

$$-\begin{Bmatrix} F_X \\ F_Y \end{Bmatrix} = \begin{bmatrix} K_{XX} & k_{XY} \\ k_{YX} & K_{YY} \end{bmatrix} \begin{Bmatrix} x \\ y \end{Bmatrix} + \begin{bmatrix} C_{XX} & c_{XY} \\ c_{YX} & C_{YY} \end{bmatrix} \begin{Bmatrix} \dot{x} \\ \dot{y} \end{Bmatrix} \tag{1}$$

The stiffness and damping coefficients are related to the gas properties and to the geometrical constraints imposed by the seal and rotor surfaces, and are strongly frequency dependent (Kleynhans and Childs, 1997; Childs and Wade, 2004). A radial displacement of the shaft 'pushes' the gas molecules in front of it, and this transmission of motion is neither instantaneous nor frictionless; the shaft therefore experiences a resistance along the direction of the displacement (direct stiffness *K*) and a partial dissipation of its kinetic energy by viscous friction (direct damping *C*). If the gas is rotating in the plane *X, Y* then also cross-coupled coefficients *k* and *c* are generated; the representation of Fig. 1 can help to visualize their physical meaning.

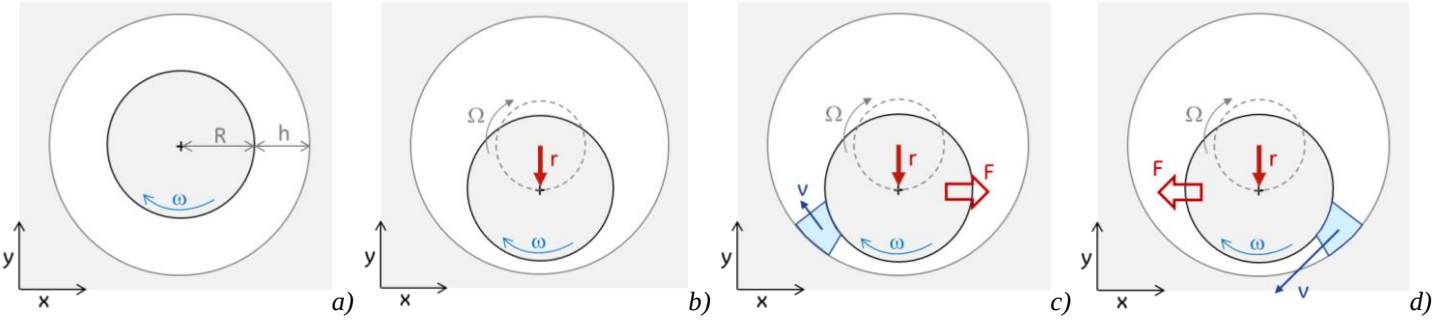

Figure 1. 2-D schematic view of the annular gap between rotor and seal: (a) no offset (zero-amplitude precession orbit); (b) shaft rotating at speed ω and orbiting at speed Ω; (c) gas volume rotating at average velocity v/R lower than Ω: the shaft "pushes forward" the gas; (d) gas volume rotating at average velocity v/R higher than Ω: the shaft is "pushed" by the gas along its orbit.

The sketch in Fig.1a represents a shaft with radius R rotating around its axis with angular velocity ω, inside a seal with inner radius $R+h$. In Fig.1b the shaft is also revolving around a vibration axis, with angular velocity Ω. A forward whirl orbit is assumed, i.e., ω and Ω have the same sign. Due to the shaft radial displacement $\boldsymbol{r}$, the seal clearance is not uniformly equal to h but has a minimum section, where the clearance is h-r; the angular position of this minimum section changes with the same precession velocity Ω of the shaft orbit. The parameter λ is defined as the ratio between the angular velocity Ω_G of the gas in the seal clearance and the precession velocity Ω:

$$\lambda = \Omega_G / \Omega \tag{2}$$

Two main scenarios are possible depending on the value of λ:

$\lambda < 1$ The gas is rotating slower than the shaft orbit; this means that the shaft has to 'push' the gas tangentially as a consequence of its radial displacement, as shown in Fig.1c. The cross-coupled coefficients k and c represent this situation: if the shaft moves along the x axis, thus reducing the seal clearance in that direction, it is subject to a force in the y direction, caused by the resistance of the gas. A part of the shaft's kinetic energy is transferred to the gas, and another part is lost through friction losses. Therefore the gas has a stabilizing effect on the rotor, subtracting energy from its vibration.

$\lambda > 1$ The gas is rotating faster than the shaft orbit (Fig.1d), so the shaft is pushed along the tangential direction by the gas. Here the shaft is gaining kinetic energy, therefore the effect is destabilizing.

Effective means of reducing λ at the inlet of rotor-stator seals include the application of shunt holes (Memmott, 1994) and swirl brakes (Iwatsubo and Iwasaki, 2002) to decrease the tangential gas velocity Ω_G.

The dynamic stiffness of a simplified (concentrated-parameters) system described by Equation (1) results from a sum of vectors that is graphically represented in Figure 2. The vibration amplitude of the rotor is equal to the exciting force $\boldsymbol{F}$ divided by K_{dyn}, therefore the dynamic stiffness of the system needs to be maximized in order to improve the rotordynamic behavior of the compressor. The condition of rotordynamic instability corresponds to K_{dyn} approaching zero.

The vector plot clearly shows the contribution of each stiffness and damping coefficient to the overall dynamic stiffness. Increasing the direct coefficients K and C results in an increase of K_{dyn}, while increasing the cross-coupled stiffness k and the swirl parameter λ has the effect of reducing K_{dyn}.

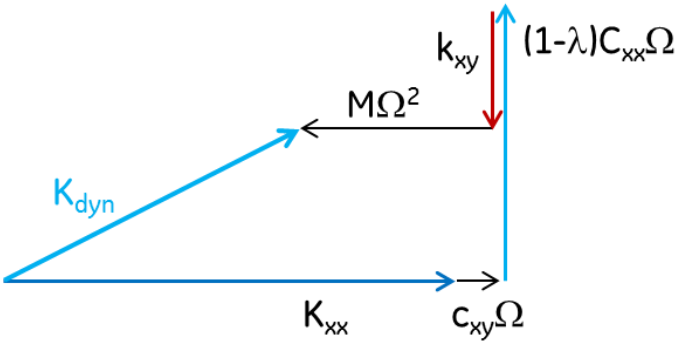

Figure 2. Vector diagram showing the components of the dynamic stiffness K_{dyn}. The diagram is referred to direction x; the analogous diagram referred to axis y is tiled by 90° and is obtained by swapping all the indices x and y.

Basing on the above considerations, a rotor-stator seal should be characterized by high K, C, c and low k, λ to minimize rotor vibrations, with particular reference to the synchronous coefficients (since most rotor exciting forces, and namely the residual unbalance, are synchronous with the rotating speed). Extending the analysis to include all the effects on the rotordynamic behavior of the compressors, this wish list can be further refined: while a high damping is positive under all points of view, a high direct stiffness can significantly alter the critical speeds of the rotor, in terms of frequency and mode shape. If the value of K is function of the operating conditions, this variability could have undesired effects. For example, one or more critical speed peaks may shift inside the operating speed range; even worse, a significant change of mode shape might lead to high vibrations due to rotor unbalance: the set of masses applied to the rotor during a high speed balancing can become less effective in reducing its vibrations if the mode shape is altered, and ultimately might cause an increase of vibrations. For this reason the ideal seal would have coefficients C, c as high as

possible and k, λ as low as possible, while K should be as high as possible to increase the dynamic stiffness without causing significant alterations of the rotordynamic of the system.

Damper seals were introduced to enhance the rotordynamic stability of centrifugal compressors, by achieving one or more of the purposes listed above (Moore et al., 2002). This term is commonly referred to several kinds of devices, including honeycomb seals (Memmott, 1994; Zeidan et al., 1993), hole pattern seals (Yu and Childs, 1998), pocket seals (Richards et al., 1995). In particular, due to their geometry honeycomb and hole pattern seals can develop high dynamic stiffness coefficients, while this is not the case for pocket damper seals, whose dynamic coefficients have the same order of magnitude of traditional labyrinth seals.

This work and the case studies here presented refer to honeycomb seals, but all the main considerations can be extended to other types of damper seals. Honeycomb cells are typically obtained by spark erosion or by brazing on the inner surface of a seal ring, with the use of carbon steel, stainless steel or aluminum alloy as base material. Figure 3 shows a honeycomb seal for a high pressure centrifugal compressor; shunt holes are visible on the upstream side of the seal (Memmott, 1994).

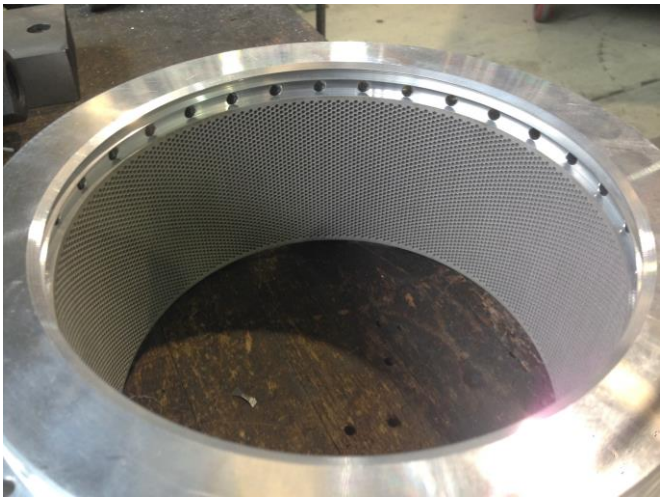
a)


b)

Figure 3. a) Honeycomb seal, electro-discharge machined from an aluminum alloy single block. b) Detailed view of the seal surface. Shunt holes are visible on the top side.

Honeycomb seals are commonly used on high pressure compressors because they have a much better overall effect on stability with respect to labyrinth seals of equivalent geometry (length, diameter, clearance) and no impact on compressor efficiency, due to their good sealing performance (see (Childs et al., 1989) for a comparison between honeycomb and labyrinth seal leakage flowrate). The reason of the better stability effect is that, even if a honeycomb generally has higher cross-coupled stiffness than a labyrinth, its synchronous direct stiffness K and damping C are much higher than for labyrinth seal (Vannini et al., 2011). Such stiffness and damping properties are related to the circulation of the gas inside the cells of the stator surface. Within some approximation, each cell can be viewed as a spring and a damper acting in parallel, since a displacement of the rotor causes a compression of the gas contained in the cell (generating a resistive force, experienced as a radial stiffness by the rotor) associated to a recirculation (viscous dissipation, with damping effect). Due to its 'rough' surface, a honeycomb seal is also much more effective in reducing λ than a labyrinth seal: the tangential motion of the gas is slowed by friction on the stator surface.

Unfortunately it is not possible to selectively maximize the damping of a honeycomb seal without increasing its direct stiffness, as shown in the next section. Therefore honeycomb seals on high-pressure centrifugal compressors are generally characterized by a high K that can reach the same order of magnitude of the stiffness of the journal bearings, with meaningful rotordynamic impacts that have been studied and verified experimentally (Fulton and Baldassarre, 2007; Baldassarre et al., 2014). The present study addresses the optimization of the system composed by rotor, journal bearing and honeycomb seal, through the analysis of two case studies. The calculation tool used for the analyses presented in the next sections is Isotseal™, a software tool based on a two-control-volume model developed by Texas A&M University and described in (Kleynhans and Childs, 1997), whose results are validated by comparison with experimental data (Childs and Wade, 2004; Vannini et al., 2011).

Honeycomb seal stiffness and damping as function of design parameters

The dynamic coefficients of a honeycomb seal are function of a large number of geometrical and thermodynamic parameters. In general the process parameters are not directly manageable during the design phase (pressures, gas density and molecular weight, gas

viscosity), while the seal geometry can be optimized to obtain the design targets in terms of rotordynamic stability, compressor leakage and performance.

The effects of the differential pressure across seal and of the gas density in the annular clearance are similar, as they are strictly dependent; their increase causes an increase of the seal stiffness and damping. The effect of gas viscosity on honeycomb stiffness and damping is almost negligible at all rotor speeds, even if it is included in the seal modeling.

The effects of the main geometrical parameters of the seal on its dynamic coefficients are described in detail in the following plots (Figures 4 to 8), obtained from a sensitivity analysis performed with Isotseal™ code on a reference high-pressure compressor processing natural gas. The analyzed parameters include the width and tapering of the clearance, axial length of the seal, the dimension of the cells and the inlet swirl ratio of the gas leakage. ±20% variations were applied for the purpose of the analysis.

Seal clearance tapering (Figure 4): starting from a baseline seal with cylindrical clearance (tapering = 0), the clearance was increased alternatively on the HP side (convergent clearance, tapering >0) and on the LP side (divergent clearance, tapering <0). An increase of tapering leads to an increase of *K* and a decrease of *C*, with a small effect on cross-coupled terms. In particular the negative *K* associated to divergent honeycomb tapering causes a strong reduction of K_{dyn}, that may lead to catastrophic effects on compressor stability (Camatti et al., 2003).

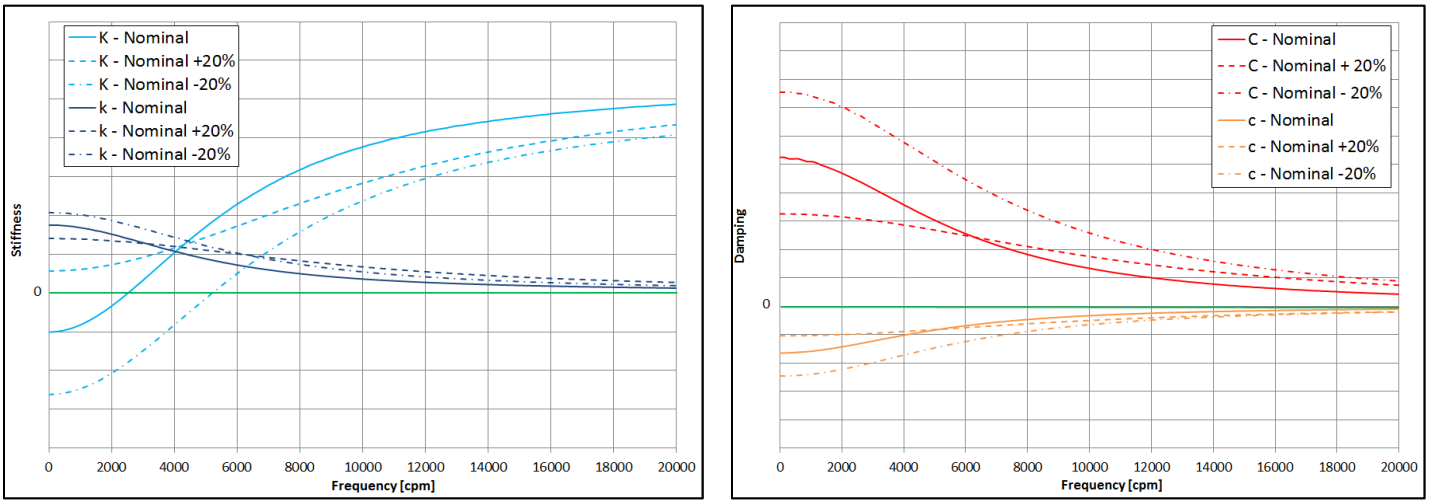

Figure 4. Honeycomb stiffness and damping sensitivity to seal tapering variations

Cell depth (Figure 5): The main effects are related to direct stiffness and damping: honeycomb cells can be seen as springs, whose stiffness decreases when their length (i.e. the cell depth) is increased. Moreover, deeper cells corresponds to a higher macroscopic roughness of the seal inner surface; this reduces *k* (by reducing the tangential velocity of the gas, see Figure 1) and therefore has a stabilizing effect. The effect of cell depth on leakage flowrate is not straightforward and test results are quite controversial, with instances showing a leakage decrease in case of shallower cells (Childs et al., 2013), other presenting a leakage decrease in case of deeper cells (Holt and Childs, 2002), and even references showing non-monotonic trend of the leakage vs. cell depth (Li et al., 2010).

Honeycomb seal length (Figure 6): Variations of seal length have a roughly proportional effect on *K* and *C*, as for a fluid dynamic journal bearings. Also the cross coupled stiffness *k* is impacted; the reason is that the gas takes more time to flow through a longer seal, and therefore undergoes a larger acceleration (or deceleration, depending on the inlet swirl value) in the tangential direction, due to friction with the rotor and stator surfaces.

Honeycomb seal average clearance (Figure 7): The main effect of a clearance reduction is an increase of direct stiffness *K* and direct damping *C* (in analogy to the effect of a clearance reduction on a fluid dynamic journal bearing); *k* and *c* are almost unchanged, at least in the higher frequency range.

Inlet swirl ratio (Preswirl) (Figure 8): this parameter can be modified by applying devices like swirl brakes and shunt holes. The variation of the preswirl affects the cross-coupled coefficients, while the direct coefficients are almost unchanged. In particular a higher preswirl is associated to higher *k* and lower *c*; this has a destabilizing effect, as discussed before. The limited variation of *k* and *c* in these example plots is due to the fact that the ±20% factor corresponds in absolute terms to small changes of inlet swirl.

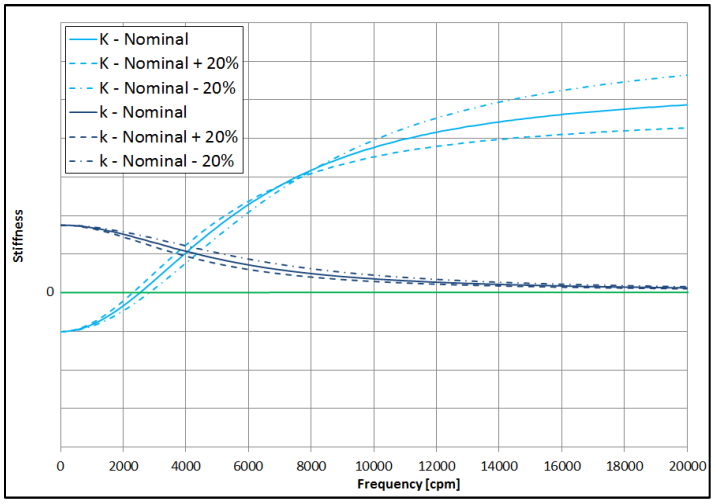

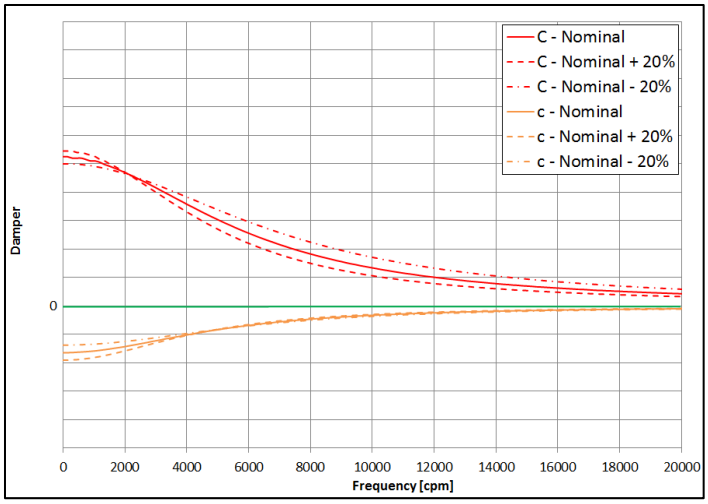

Figure 5. Honeycomb stiffness and damping sensitivity to cell depth variations

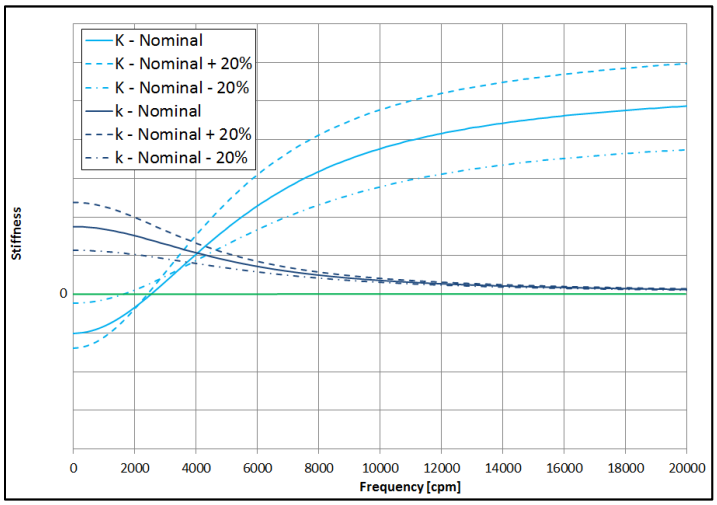

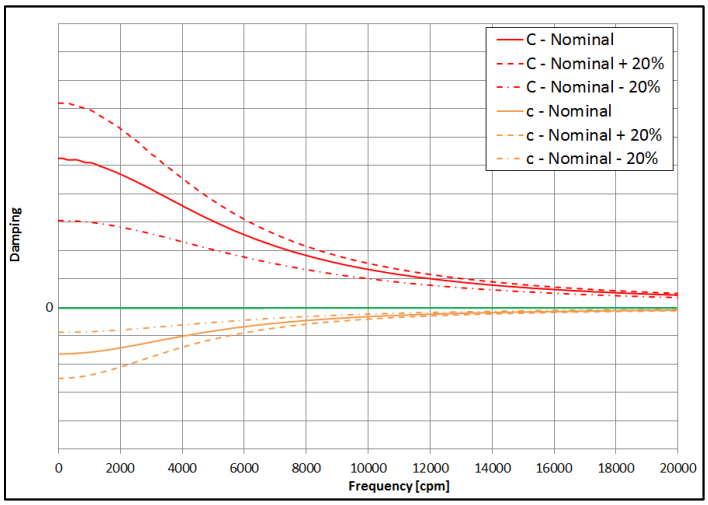

Figure 6. Honeycomb stiffness and damping sensitivity to seal length variations

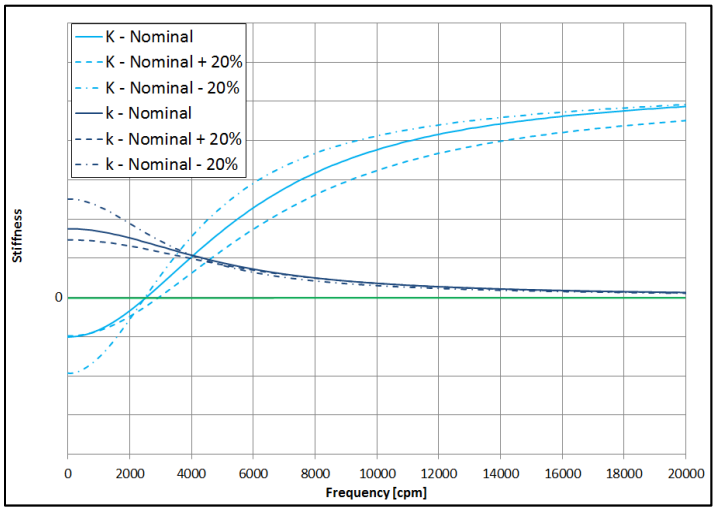

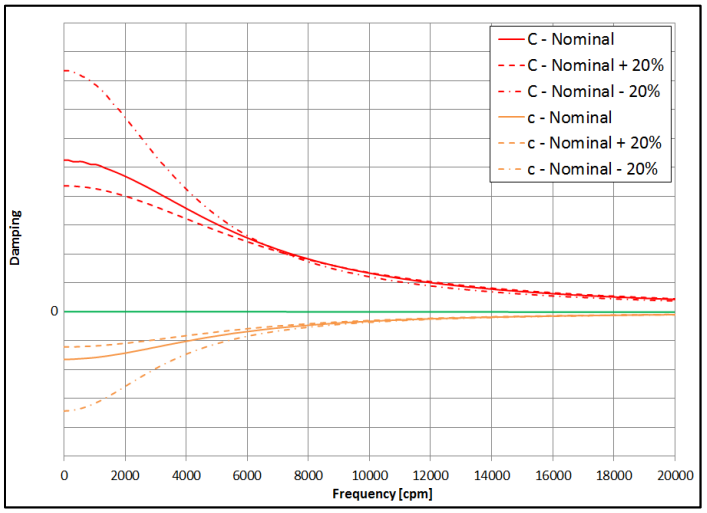

Figure 7. Honeycomb stiffness and damping sensitivity to seal average clearance variations

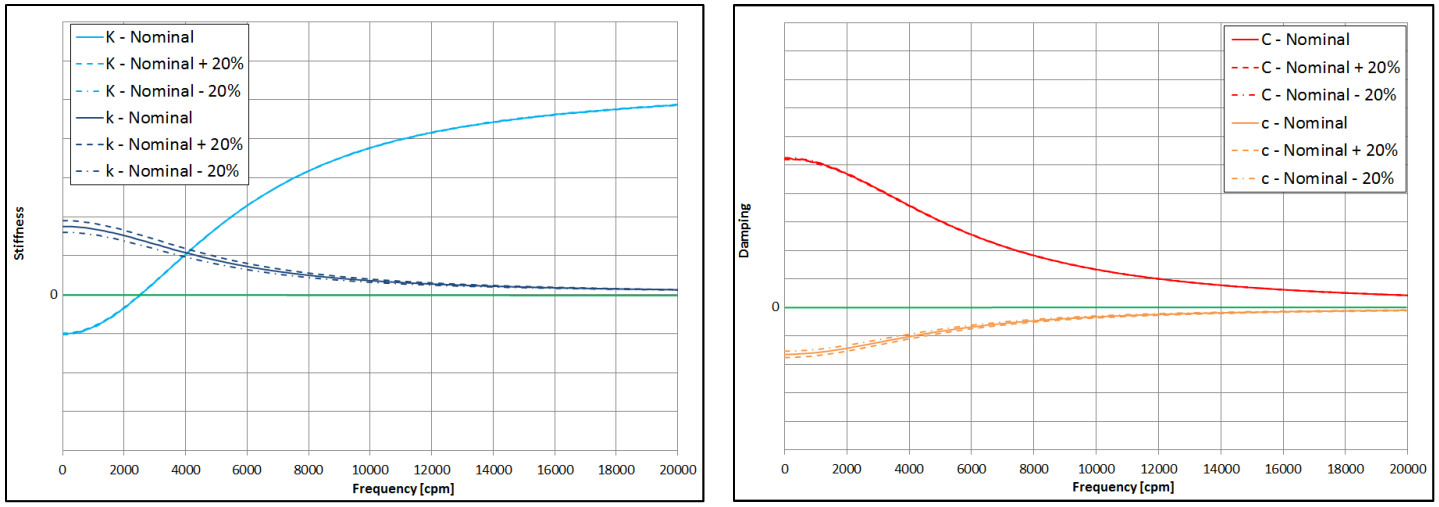

Figure 8. Honeycomb stiffness and damping sensitivity to seal inlet swirl ratio variations

The above plots show the complex interdependence between the dynamic coefficients of a honeycomb seal and its geometric parameters. Any dimensional variation has an impact on the seal stiffness, damping, leakage flowrate and therefore on the rotordynamic and thermodynamic performance of the compressor. The design of a honeycomb seal shall be aimed to obtain the all the features listed as comment to Figure 2 (C, c as high as possible; k, λ as low as possible; K high but limited to reduce impact on response to unbalance and mode shapes) with particular focus on synchronous coefficients, but the multiplicity of the targets and the complex correlation between input and output variables require to accept some trade-offs, identifying an optimum compromise solution. In particular the primary targets of strong stabilizing effect and low impact on efficiency can generally be achieved on a high-pressure compressor only by a seal with very large direct stiffness K. This is exemplified by the case studies reported in the next section, and bears important consequences on the rotordynamic design of the compressor.

ANALYSIS OF CASE STUDIES

The rotordynamic behavior of high-pressure centrifugal compressors equipped with honeycomb seal on balance drum was analyzed through two case studies, whose features allowed to clearly evaluate the interplay between journal bearing and honeycomb stiffness. The two compressors have very similar geometry and operating conditions (see Figure 9 and Table 1 for comparison), but significantly different journal bearing stiffness and damping (Table 2) due to the selection of different clearance and preload values.

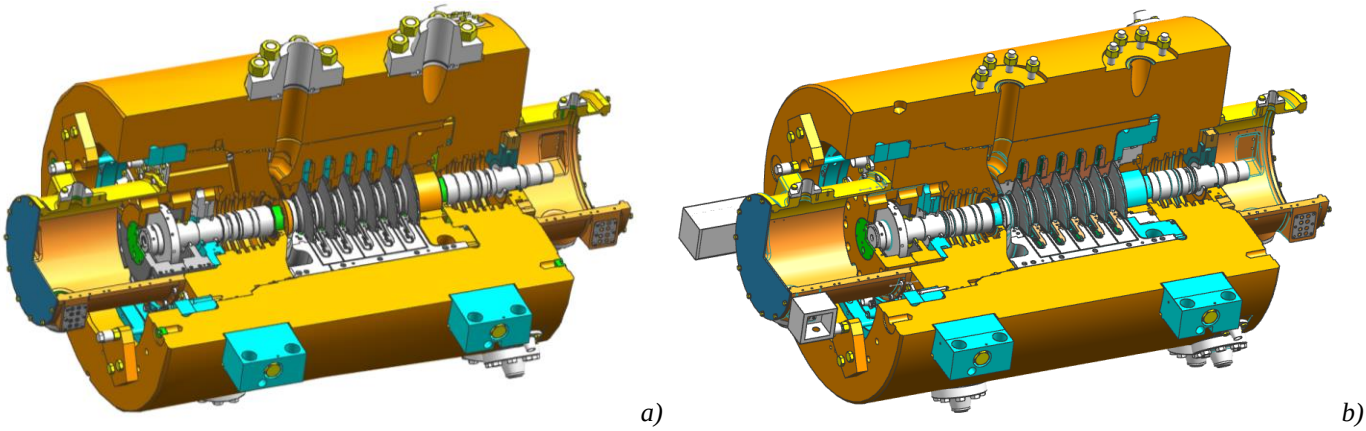

a) *b)*

Figure 9. a) 3D view of Unit A centrifugal compressor. b) 3D view of Unit B centrifugal compressor.

		Unit A	Unit B
Casing Type	[-]	Barrel	Barrel
Number of Stages	[-]	6	6
Impeller Max External Diameter	[mm]	318	310
Rotor Weight	[kg]	246	239
Bearing Span	[mm]		
NC1	[rpm]	6712	7252
Rated Speed	[rpm]	10,857	11,080
Rated Suction Pressure	[bar-A]	250	213
Rated Discharge Pressure	[bar-A]	550	550
Rated Mass Flow	[kg/sec]	59.8	45.7
Gas Molecular Weight	[kg/mol]	21.7	26.3
Journal Bearings Size	[mm]	90	90
Journal Bearing Clearance (normalized)	[-]	1	0.86
Journal Bearings Type		Flooded, Tilting Pad	Flooded, Tilting Pad
Honeycomb Seal Length vs Diameter ratio	[-]	0.529	0.541
Average Honeycomb Seal Clearance (normalized)	[-]	1	1.11
Honeycomb Seal Cell Depth (normalized)	[-]	1	0.78
Honeycomb Seal Cell Width (normalized)	[-]	1	1

Table 1. Main features of the two compressors used as case studies.

	K_{JB}	k_{JB}	C_{JB}	c_{JB}
	[normalized]		[normalized]	
Unit A	3.1 E-01	1.1 E-03	2.1 E-04	3.5 E-07
Unit B	6.8 E-01	1.0 E-03	4.4 E-04	3.1 E-07

Table 2. Journal bearing coefficients calculated at MCS, for the two case studies (values averaged between DE and NDE sides). The values of Tables 2-3-4 are normalized to 1.

No load test data

In no-load condition (mechanical running test under vacuum), where the honeycomb seal has negligible effects, the rotordynamic behavior of the two compressors was quite similar (Figure 10). The 1st critical speed peak frequency is slightly lower for *Unit A* than for *Unit B* (about 6500 rpm vs. 7500 rpm), due to the lower stiffness of the bearings and to the longer bearing span (see Table 1). The amplification factor (*AF*) of the first critical speed, calculated from the Bode plots, is about 3.5 for *Unit A* and about 4.7 for *Unit B*.

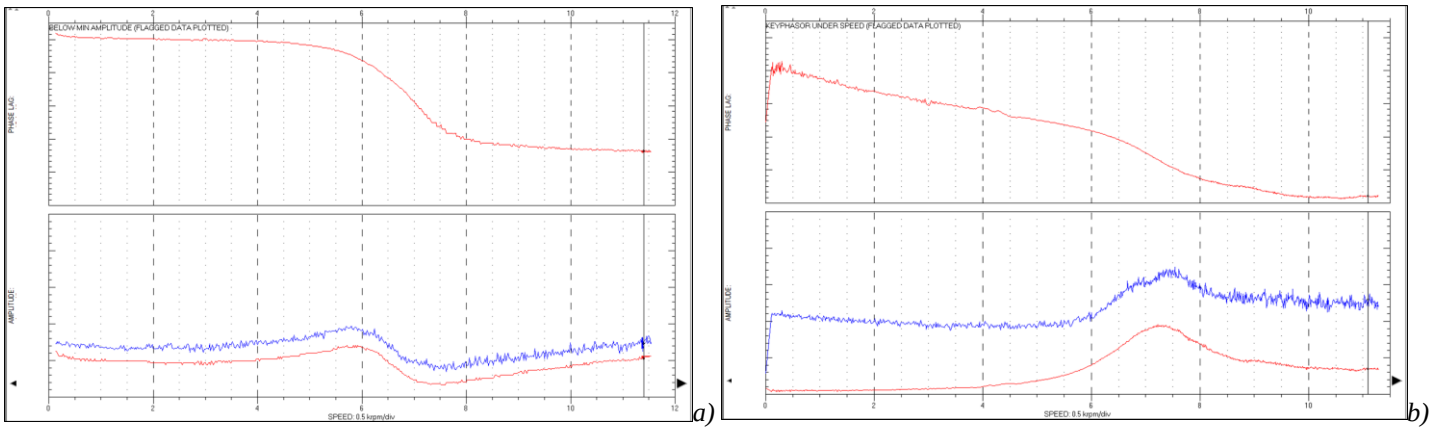

a) b)

Figure 10. a) Bode diagram of a radial probe on DE side of Unit A, during a ramp-up in MRT. b) Bode diagram for Unit B (same probe and same scale). The vibration levels are very similar; the 1st critical speed is higher for Unit B, due to the stiffer bearings.

Full load test data

The two compressors were tested in Full Speed, Full Load, Full Pressure condition (*FSFLFP*) on the same test bench, using the same driver (shop electric motor). In full load condition, where the radial stiffness and damping of the honeycomb seal are fully developed, the two compressors showed largely different vibration: similar to no load conditions for *Unit A*, much higher than in no load condition for *Unit B* (see comparison between Figure 10 and 13).

Figures 11 and 12 show the trends of rotating speed and suction pressure respectively, recorded during the tests. *Unit A* was carried to MCS in less than 30 minutes, regulating the inlet gas flowrate to approach the left limit of the curve, and then gradually pressurized, thus increasing the absorbed power up to a maximum value at the end of the recording. *Unit B* was also carried quickly to MCS speed and positioned close to the left limit of the curve, but the inlet pressure remained roughly constant during the test, therefore the absorbed power varies only with speed.

Both *Unit A* and *B* reached full load conditions: in the final part of trend for *Unit A* and in the first half of the trend for *Unit B*.

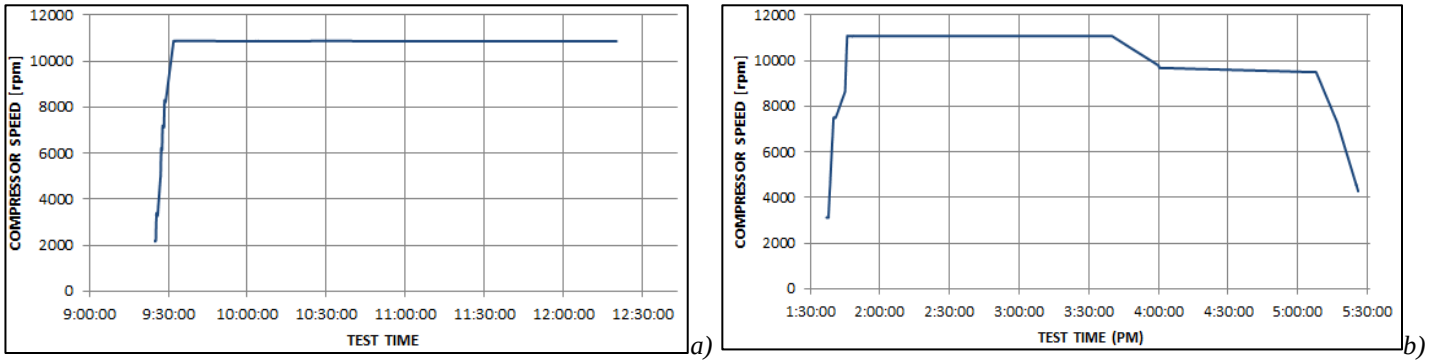

Figure 11. a) Compressor speed vs time trend diagram during FSFLFP test of Unit A. b) Same diagram for Unit B.

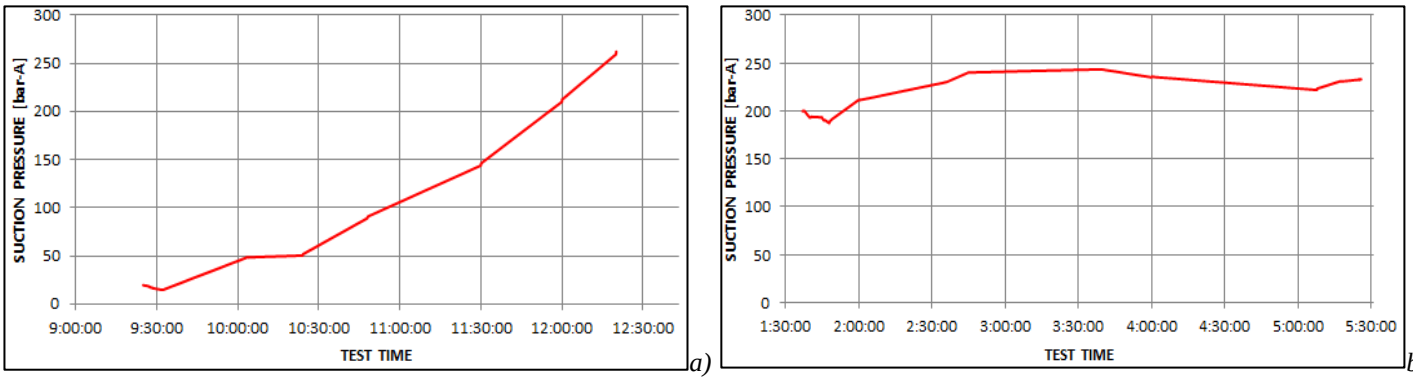

Figure 12. a) Compressor suction pressure vs time trend diagram during FSFLFP test of Unit A. b) Same diagram for Unit B.

Figure 13 shows the comparison between the vibration trends (amplitude and phase) of the two units during the test intervals referred in Figures 11-12. For the sake of clarity the vibrations of a single radial probe out of 4 are plotted, anyway all the probes of a single unit show a qualitatively similar behavior.

Although the amplitude of radial vibrations was within the contractual limits for both compressors, the synchronous vibration of *Unit A* showed a marked dependence on process conditions (operating speed, inlet gas flowrate, suction pressure), compared to a relatively insensitive behavior of *Unit B.* In particular for a similar increase of compressor suction pressure from 200 to 250 bar-A, *Unit A* experienced (from 11h50' to 12h20') an increase of vibration amplitude three times higher than *Unit B* (from 1h55' to 3h40'), and a phase shift almost two times larger.

The high sensitivity of *Unit A* to honeycomb effect with respect to *Unit B* is even more evident when comparing the vibrations in no load condition (Figure 10) to those in load conditions (Figure 13). Such a comparison shows that, at MCS, the synchronous vibration amplitude of *Unit A* is six times higher at full load than at no load, while for *Unit B* the amplitude is just two times higher.

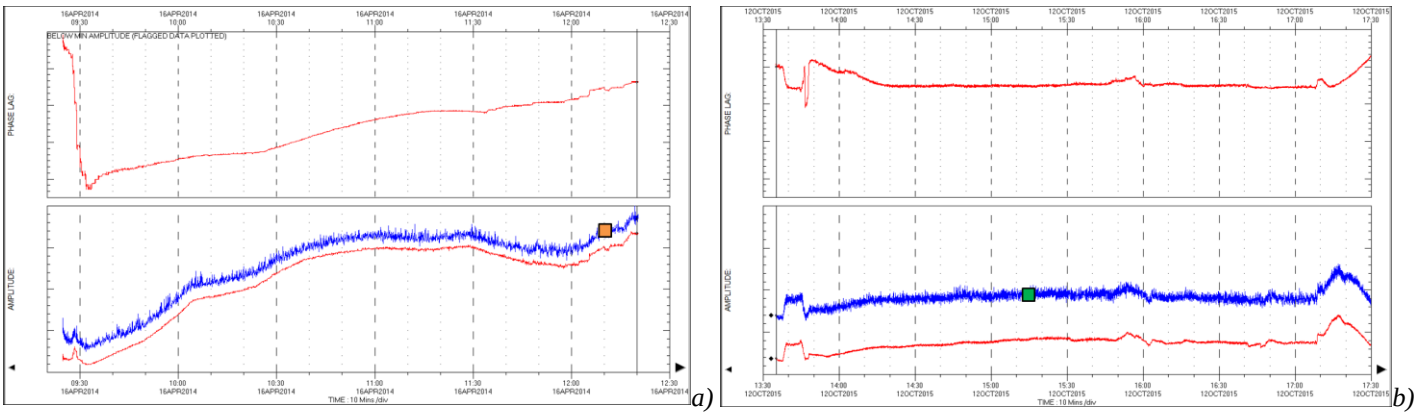

a) b)

Figure 13. a) Vibration vs time trend diagram of a single radial probe out of 4 during FSFLFP test of Unit A. b) Same diagram for Unit B, with same y axis scale. The initial variations up to 13h45' in Figure b) are due to startup transients.

The Bode plots recorded during the startups of the full load tests (Figure 14) compared to those measured in no-load test (Figure 10) confirm the dependency of vibrations on load condition due to the effect of the honeycomb seal. The peak frequency of the first critical speed observed during no-load tests is shifted to higher frequencies in load conditions, mainly due to the stiffness developed by the honeycomb seal. For *Unit A* the frequency increases by 3%, versus a 14% increase on *Unit B*. The reason of this difference is that the startup of *Unit A* occurred at relatively low pressure (Figure 12a), so with small difference with the no load case, while the startup of *Unit B* occurred at high pressure (Figure 12b) inducing a significant honeycomb effect.

The damping effect of the honeycomb on the first critical speed is also clearly visible, as a reduction of the amplification factor: during the *FSFLFP* test the first critical speed peak of both compressor was overdamped according to API617 definition (*AF* <2.5), to be compared with the values of 3.5 and 4.7 mentioned above for the no-load test.

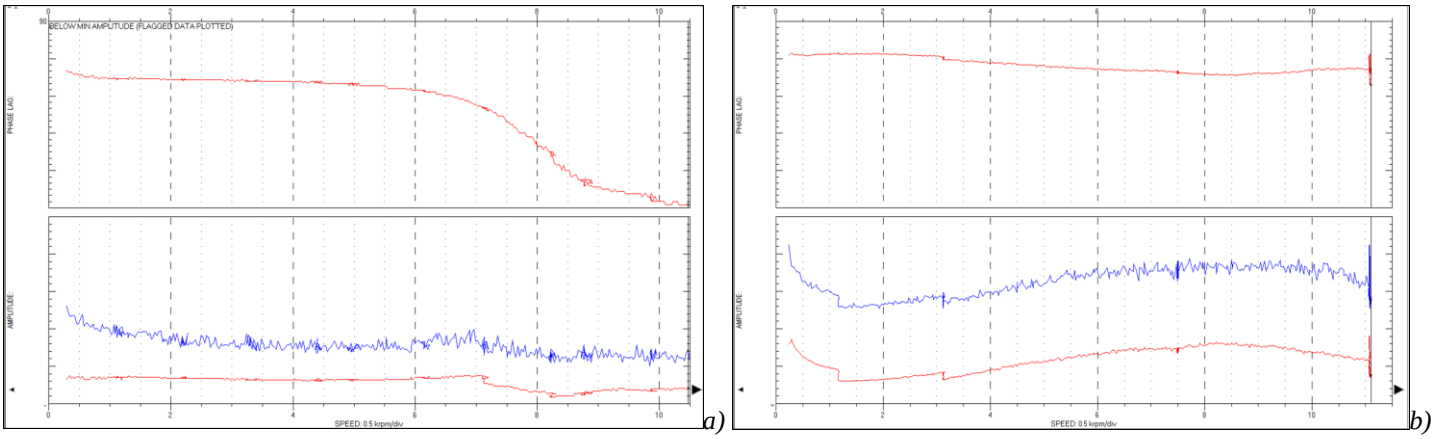

a) b)

Figure 14. a) Bode diagrams of a radial probe on NDE side of Unit A, during FSFLFP test. b) Same diagram for Unit B.

The dynamic coefficients of the two honeycomb seals were calculated with Isotseal™ software in *FSFLFP* test conditions. The output values, relative to MCS (synchronous coefficients) are summarized in Table 3. The stiffness coefficients *K*, *k* are quite similar for the two units, while the direct damping *C* of *Unit B* seal is significantly higher (+50%) than for *Unit A*. The cross-coupled damping *c* is always very low compared to the other coefficients and is therefore negligible for practical purposes; it is reported in Tables 2-3-4 only for completeness. The differences in dynamic performances are mainly due to the different geometric parameters of the seals and to the different test gas composition (see Table 1).

A comparison between the journal bearings dynamic coefficients (Table 2) and the honeycomb seals dynamic coefficients (Table 3) shows that both direct and cross-coupled stiffness of the seals are higher than those of the journal bearings, while in terms of direct damping the journal bearings are more performing than the honeycomb seals. Labyrinth seals with the same dimensions and operating conditions would have a stiffness K_{LS} lower by one order of magnitude (see Table 4 vs. Table 3); as a consequence they would provide an insufficient stabilizing effect, delivering also lower damping.

	K	k	C	c
	[normalized]		[normalized]	
UNIT A	9.4 E-01	8.3 E-02	1.5 E-04	9.1 E-05
UNIT B	1.0 E+00	9.6 E-02	2.3 E-04	1.0 E-04

Table 3. Calculated synchronous honeycomb seal coefficients for the two case studies, at MCS in full load condition.

	K_{LS}	k_{LS}	C_{LS}	c_{LS}
	[normalized]		[normalized]	
UNIT A	6.7 E-02	5.6 E-03	5.3 E-05	3.5 E-05
UNIT B	1.3 E-01	3.1 E-02	1.3 E-04	6.8 E-05

Table 4. Labyrinth seal dynamic coefficients for the two case studies, calculated in the same conditions of values at Table 3.

JOURNAL BEARING OPTIMIZATION TO MITIGATE THE VIBRATION RISK DUE TO HONEYCOMB SEAL

The analysis of the two case studies clearly shows the variation of radial vibrations between no load and load conditions, mainly determined by the aerodynamic effects associated to the honeycomb seal. It also highlights the influence of the journal bearing stiffness that represents the main difference between the two otherwise similar compressors: the variation of rotor vibrations is higher for *Unit A*, equipped with softer journal bearings. This is intuitive when considering that the honeycomb seal in load conditions acts as a sort of third journal bearing, and therefore its effect on rotor vibrations is expected to increase with the ratio between its dynamic coefficients and those of the bearings.

First level assessment (reference check)

A larger set of 20+ references (high-pressure centrifugal compressors equipped with honeycomb seal, tested at full load) was analyzed in addition to the two case studies discussed above, with the purpose of identifying some general assessment criteria for the sensitivity of rotor vibrations to the interaction between honeycomb seal and journal bearings.

The ratio between journal bearings and honeycomb seal direct synchronous stiffness was calculated for each reference and plotted on a diagram (Figure 15). Each value was calculated at MCS and at the left limit of the operating curve. The positions of *Unit A* and *Unit B* are also indicated; they are relevant to the *FSFLFP* data points shown by markers in Figure 13. The bearing direct stiffness K_{JB} of *Unit A* is about half of *Unit B* (Table 2), while the honeycomb seal direct stiffness K is similar between the two units (Table 3).

In the diagram of Figure 15 a fixed ratio K_{JB}/K is represented by a line passing through the origin. A threshold value for the K_{JB}/K ratio can be defined to enclose all the references that showed low or no vibration sensitivity to honeycomb seal operating conditions; conservatively this threshold is here shown as the dashed red line in figure, in absence of further low-sensitivity references closer to *Unit A*. A simple design rule for high pressure compressors can be defined by imposing that the corresponding point on the diagram shall fall above the red line. If this check is not verified, the design parameters of the journal bearings (generally their clearance and preload) and the geometry of the honeycomb seal shall be properly tuned, compatibly with the constraints imposed by the other rotordynamic requirements listed in (API617).

Second level assessment (detailed rotordynamic calculation)

The check of the journal bearing vs. honeycomb seal stiffness represents a first step for the risk assessment of vibration increase in load conditions. If a more accurate evaluation is required, the second step is to directly calculate the influence of the honeycomb seal on compressor vibrations, by comparing the rotor response to unbalance with and without the honeycomb dynamic coefficients; a procedure to perform this calculation is described in (Baldassarre et al., 2014). The amplitude and phase of the synchronous rotor vibration shall be calculated at the radial probe locations as shown in Figure 16, for a given unbalance mass set (e.g. the one prescribed by API617 for the response to unbalance calculation).

Figure 17 shows the results of such calculations for *Unit A* and *B* respectively. The plots show that for *Unit A* the phase lag φ between DE and NDE synchronous vibration is strongly altered by the presence of the honeycomb: the lag is φ_{NL} = 2.2 degrees in no load condition and becomes φ_{L} = -152.6 degrees in load condition.

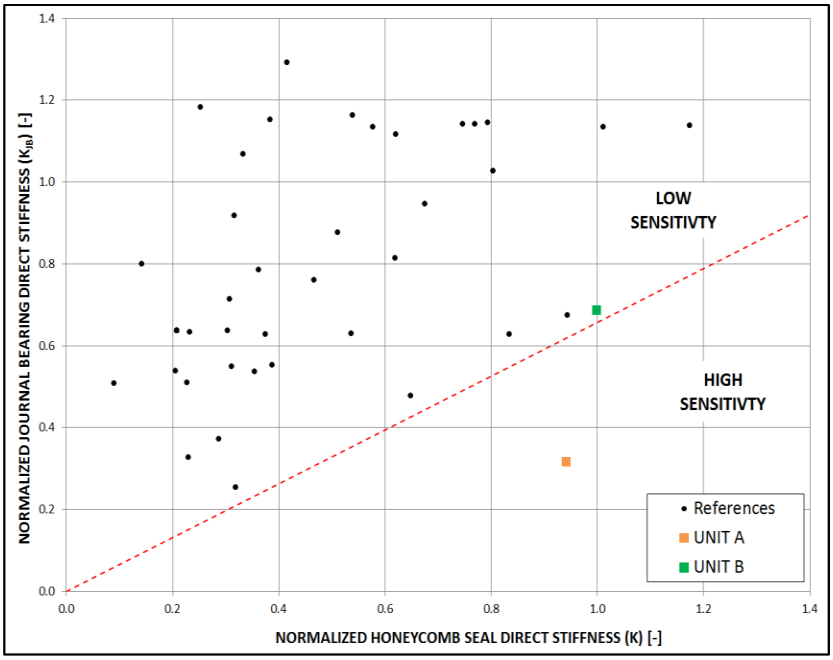

Figure 15. Honeycomb seal normalized direct stiffness vs journal bearing normalized direct stiffness for reference high pressure compressors. Both coefficients are calculated at MCS & surge limit, for synchronous vibration.

The relative phase shift $\Delta\varphi$, defined as:

$$\Delta\varphi = \varphi_{NL} - \varphi_L \tag{3}$$

is equal to 154.8 degrees. On *Unit B* the variation of the DE-NDE phase lag between no load and load condition is much smaller: $\Delta\varphi$ = 18 degrees, due to the the variation from φ_{NL} = 1.2 degrees to φ_L = -16.8 degrees.

The larger is the phase shift $\Delta\varphi$, the higher is the sensitivity of rotor vibrations to the effect of the honeycomb. The reason is that the residual unbalance of the rotor, that is continuously distributed (in modulus and phase) along its whole length, is corrected during the balancing phase by adding discrete masses at few locations along the rotation axis. The rotor balancing procedure, that is carried out in no-load conditions, allows to find a set of balancing masses whose weight and angular position can compensate the rotor unbalance and therefore minimize the radial vibrations. The phase variation caused by the honeycomb in load conditions is not uniform along the rotor ($\Delta\varphi \neq 0$), therefore it modifies the relative phase angles between the (discrete) correcting masses and the (continuous) residual unbalance distribution. This relative phase shift can modify the resultant unbalance vector, reducing the effectiveness of the rotor balancing and leading to increased rotor vibrations.

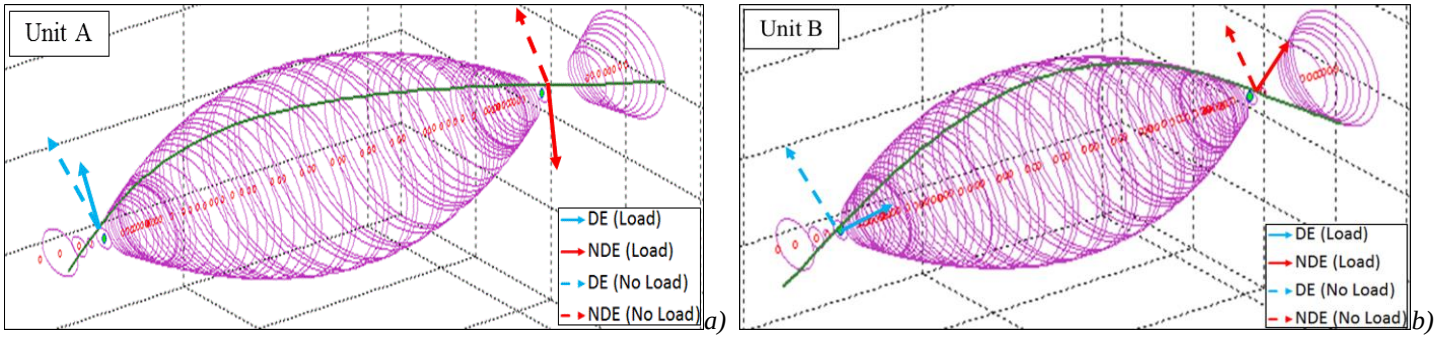

a) *b)*

Figure 16. 3D representation of the synchronous radial vibration vectors, on DE and NDE sides

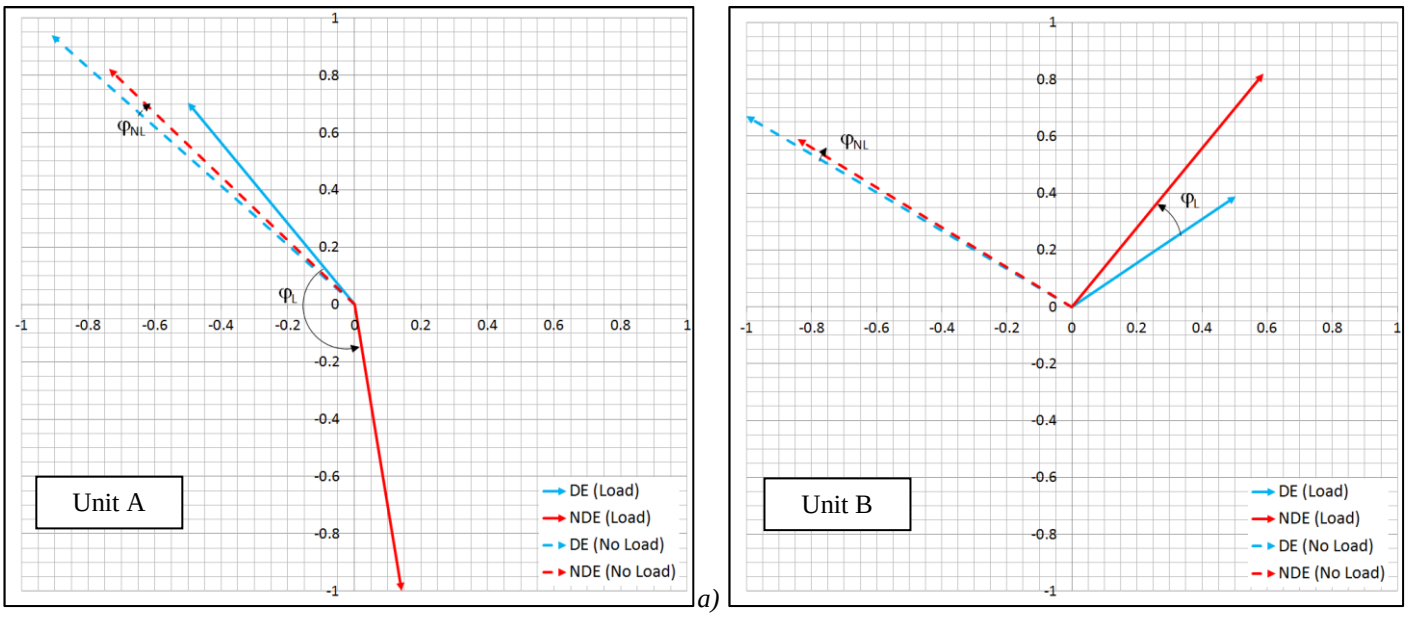

Figure 17. Synchronous radial vibrations of Unit A and Unit B in load (continuous arrows) and no load condition (dashed arrows). The vectors represent the vibration (normalized) amplitude and phase, evaluated at MCS. The load conditions considered for the calculations are those marked by the squares in Figure 13.

This kind of rotordynamic analysis can be performed during the design phase, to evaluate in a quantitative way the sensitivity of the rotor vibrations to the presence of the honeycomb. A maximum limit can be imposed on the phase variation $\Delta\varphi$ between rotor ends caused by the aerodynamic load, and can be achieved by properly tuning the design of the rotor, the journal bearings and the honeycomb seal.

CONCLUSIONS

The rotordynamic behavior of centrifugal compressors equipped with honeycomb seal on the balance drum is altered by the additional stiffness and damping associated to the seal in load conditions; on high-pressure compressors the direct stiffness of the honeycomb seal may be close or even higher than the direct stiffness of the journal bearings. The aerodynamic effect of this seal can induce significant changes in the peak frequency and amplitude of critical speeds and in the associated mode shapes. As a consequence the amplitude and phase of the vibrations measured by the radial probes may undergo significant variations, depending on the aerodynamic load of the compressor. Such vibration changes were analyzed and quantified for two case studies, and were put in relation with the ratio between the bearing stiffness and the honeycomb stiffness (direct synchronous coefficients, calculated at MCS and surge limit). A threshold limit on this stiffness ratio, based on references, was proposed as a first screening criterion to assess the sensitivity of compressor vibrations to load conditions. A more detailed analysis requires rotordynamic calculations to estimate the honeycomb seal effect on the synchronous rotor vibration, and specifically on the trend of the vibration phase along the axial direction. Large phase variations between no-load and load conditions may alter the relative angular position of the residual rotor unbalance and the balancing weights, thus causing a variation of the resultant vector and a potential increase of vibration levels.

The sensitivity of rotor radial vibrations to the aerodynamic effect of the honeycomb seal can be limited during the design phase, by optimizing the geometric and operating parameters of the seal and the journal bearings to keep under control the relative stiffness of the honeycomb, as far as allowed by other constraints associated to requirements on compressor layout, performance and rotordynamic behavior.

NOMENCLATURE

Acronyms

AF	Amplification Factor
DE	Drive End
FSFLFP	Full Speed, Full Load, Full Pressure
HC	Honeycomb
JB	Journal Bearing
MCS	Maximum Continuous Speed
MRT	Mechanical Running Test
NC1	First critical speed at infinite bearing stiffness
MW	Molecular Weight
NDE	Non Drive End

Symbols

C	[Ns/m]	Direct damping
c	[Ns/m]	Cross-coupled damping
F	[N]	Reaction force due to the interaction between shaft and gas volume
h	[mm]	Radial clearance between shaft and journal bearing
K	[N/m]	Direct stiffness
k	[N/m]	Cross-coupled stiffness
r	[mm]	Radial displacement of the rotor with respect to the seal/bearing axis
$\Delta\varphi$	[deg]	Phase lag between radial vibrations at journal bearings in no load and load condition
λ	[--]	Ratio between the angular speeds of the gas annulus and the shaft precession orbit
φ	[deg]	Phase lag between synchronous radial vibration at DE side and NDE side
Ω	[rpm]	Shaft precession angular speed
ω	[rpm]	Shaft rotation angular speed

Subscripts

G	Gas
L	Load
LS	Labyrinth Seal
NL	No Load

REFERENCES

API 617, 2014, "Axial and Centrifugal Compressors and Expander-Compressors for Petroleum, Chemical and Gas Industry Services", Eighth Edition, American Petroleum Institute, Washington, D.C.

Baldassarre L., Bernocchi A., Fontana M., Failli L., Mitaritonna N., Rizzo E., 2014, "Honeycomb seal effect on rotor response to unbalance", *Proceedings of the 43rd Turbomachinery & 30th Pump Users Symposia*, Texas A&M University, College Station, TX.

Camatti, M., Vannini, G., Fulton, J. and Hopenwasser, F., 2003, "Instability of a high pressure compressor equipped with honeycomb seals", *Proceedings of the 32nd Turbomachinery Symposium*, Turbomachinery Laboratory, Texas A&M University, College Station, Texas, pp. 39-48.

Childs, D., Elrod, D., and Hale, K., 1989, "Annular Honeycomb Seals: Test Results for Leakage and Rotordynamic Coefficients; Comparison to Labyrinth and Smooth Configurations," *ASME Journal of Tribology*, 111, pp. 293-301.

Childs, D. and Wade, J., 2004, "Rotordynamic-Coefficient and Leakage Characteristics for Hole-Pattern-Stator Annular Gas Seals - Measurements Versus Predictions, *ASME Journal of Tribology*, 126(2), pp. 326-333.

Childs, D., Arthur, S. and Mehta, N., 2013, "The Impact of Hole Depth on the Rotordynamic and Leakage Characteristics of Hole-Pattern-Stator Gas Annular Seals", *ASME Turbo Expo 2013*, Vol. 7A, San Antonio, TX.

Fulton, J. and Baldassarre, L., 2007, "Rotor bearing loads with honeycomb seals and volute forces in reinjection compressors", *Proceedings of the 36th Turbomachinery Symposium*, Turbomachinery Laboratory, Texas A&M University, College Station, Texas, pp. 11 to 54.

Holt, C. and Childs, D., 2002, "Theory Versus Experiment for the Rotordynamic Impedances of Two Hole-Pattern-Stator Gas Annular Seals", ASME Journal of Tribology, 124(1), pp. 137-143.

Iwatsubo, T., and Iwasaki, Y., 2002. "Experimental and Theoretical Study on Swirl Braked Labyrinth Seal", *Proceedings of the 6th International Conference on Rotor Dynamics*, Sydney, Australia, pp. 564-571

Kleynhans, G.F., Childs, D.W., 1997, "The acoustic influence of cell depth on the rotordynamic characteristics of smooth-rotor/honeycomb-stator annular gas seals", *Journal of Engineering for Gas Turbine and Power*, vol. 119, no. 4, p. 949-956.

Li, J., Kong, S., Yan, X., Obi, S. and Feng, Z., 2010, "Numerical Investigations on Leakage Performance of the Rotating Labyrinth Honeycomb Seal", *Journal of Engineering for Gas Turbines and Power*, Vol.132.

Memmott, E. A., 1994, "Stability of a High Pressure Centrifugal Compressor Through Application of Shunt Holes and a Honeycomb Labyrinth," *Proceedings of the Thirtieth Machinery Dynamics Seminar*, CMVA, Toronto, Canada, pp. 211-233.

Moore, J., Walker, S. and Kuzdzal, M., 2002, "Rotordynamic stability measurement during full-load, full-pressure testing of a 6000 psi reinjection centrifugal compressor", *Proceedings of the 31st Turbomachinery Symposium*, Texas A&M University, College Station, TX, pp. 29-38.

Muszynska, A., 2005, "Rotordynamics", CRC Press, Boca Raton, FL.

Richards, R., Vance, J., Paquette, D. and Zeidan, F., 1995, "Using a damper seal to eliminate subsynchronous vibrations in three back-to-back compressors", *Proceedings of the 24th Turbomachinery Symposium*, Texas A&M University, College Station, TX, pp. 59-72.

Vannini G., Cioncolini S., Calicchio V., Tedone F., 2011, "Development of an Ultra-High Pressure rotordynamic test rig for centrifugal compressors internal seal characterization", *Proceedings of the 40th Turbomachinery Symposium*, Turbomachinery Laboratory, Texas A&M University, College Station, Texas, pp. 46-59.

Wachel, J. C., 1975, "Nonsynchronous instability of centrifugal compressors", ASME paper 75-PET-22.

Yu, Z. and Childs, D., 1998, "A comparison of experimental rotordynamic coefficients and leakage characteristics between hole-pattern gas damper seals and a honeycomb seal", *Journal of Engineering for Gas Turbines and Power*, 120, pp.778-783.

Zeidan, F., Perez, R., and Stephenson, E., 1993, "The Use of Honeycomb Seals in Stabilizing Two Centrifugal Compressors," *Proceedings of the Twenty-Second Turbomachinery Symposium*, College Station, TX, pp. 3-15.

ACKNOWLEDGEMENTS

The authors would like to thank Mr. Marco Innocenti and Mr. Leonardo Biasci for their support during test activities and in the collection and processing of the test data used for this study.